



**HAL**  
open science

# EXPERIMENTAL STUDY ON NH<sub>3</sub>/H<sub>2</sub>/AIR COMBUSTION IN SPARK-IGNITION ENGINE CONDITIONS

Charles Lhuillier, Pierre Brequigny, Francesco Contino, Christine  
Mounaïm-Rousselle

► **To cite this version:**

Charles Lhuillier, Pierre Brequigny, Francesco Contino, Christine Mounaïm-Rousselle. EXPERIMENTAL STUDY ON NH<sub>3</sub>/H<sub>2</sub>/AIR COMBUSTION IN SPARK-IGNITION ENGINE CONDITIONS. 11th Mediterranean Combustion Symposium, Jun 2019, Tenerife, Spain. hal-02163512

**HAL Id: hal-02163512**

**<https://hal.science/hal-02163512>**

Submitted on 24 Jun 2019

**HAL** is a multi-disciplinary open access archive for the deposit and dissemination of scientific research documents, whether they are published or not. The documents may come from teaching and research institutions in France or abroad, or from public or private research centers.

L'archive ouverte pluridisciplinaire **HAL**, est destinée au dépôt et à la diffusion de documents scientifiques de niveau recherche, publiés ou non, émanant des établissements d'enseignement et de recherche français ou étrangers, des laboratoires publics ou privés.

# EXPERIMENTAL STUDY ON NH<sub>3</sub>/H<sub>2</sub>/AIR COMBUSTION IN SPARK-IGNITION ENGINE CONDITIONS

C. Lhuillier\*, P. Bréquigny\*, F. Contino\*\* and C. Mounaïm-Rousselle\*

charles.lhuillier@univ-orleans.fr

\* Université d'Orléans, France

\*\* Vrije Universiteit Brussel, Belgium

## Abstract

The mitigation of climate change implies the increasing use of variable renewable energy sources. Energy storage and transport solutions will contribute to ensure the stability, reliability and flexibility of the energy systems. Ammonia is a well-known chemical of formula NH<sub>3</sub> and, amongst other electrofuels, a promising energy carrier and carbon-free combustible fuel. Therefore, it is of significant interest to study ammonia combustion systems. The present investigation focusses on premixed ammonia/hydrogen/air combustion to assess stability ranges, performance and pollutant emissions by means of a systematic parametric study, in the purpose of optimization in the case of a current spark-ignition engine. Gaseous ammonia blends with a wide range of hydrogen fuel fractions and equivalence ratio were tested at two different loads. Results show a power output and indicated efficiency benefit of low H<sub>2</sub> enrichment for slightly rich and slightly lean mixtures, respectively. Hydrogen is therefore mainly an ignition promoter, rather than a global combustion promoter assumedly due to high thermal losses. A small amount of H<sub>2</sub>, along with supercharged operation greatly improves the performances of the engine and its stability, thus rendering NH<sub>3</sub> a very suitable fuel for SI-engines in case of in-situ H<sub>2</sub> generation. Hydrogen also mitigates unburned NH<sub>3</sub> emissions, yet not sufficiently but those could be combined with the evenly elevated NO<sub>x</sub> emissions in dedicated selective catalytic reduction systems.

## Introduction

Awareness is growing on the need to find alternatives to fossil fuels, in order to meet the carbon emission reduction targets necessary to mitigate climate change. According to the recent report [1] of the Intergovernmental Panel on Climate Change, Variable Renewable Energy Sources (VRES) should account for more than 50% of the total primary energy supply by 2050 to ensure a sustainable warming limitation.

In this new energy paradigm, energy storage and transport solutions will contribute to the efficiency and sustainability of the energy systems. The use of energy storage allows for a better resource use efficiency, and guarantees grid stability, flexibility, reliability and resilience, as a substitute to fossil fuels use [2]. It is also a major asset for the integration of VRES by smoothing the space and time mismatch between demand and supply. Electrofuels [3], i.e. fuels produced from electricity, water and any other renewable feedstock are considered promising options for energy storage and transport due to their time stability, high energy density and flexibility regarding the end-use. These properties make them particularly suitable for mid- to long-term (seasonal) energy storage, (long-distance) mobility and high-temperature heat applications.

Ammonia (NH<sub>3</sub>) is currently receiving an increased interest from industry and academia as a potential renewable carbon-free energy carrier. It is both considered as an efficient hydrogen carrier with 17.8% hydrogen content by mass and as a direct fuel for combustion or fuel cell

application. As illustrated in Table 1, ammonia can be stored in liquid form at ambient temperature under mild pressure conditions, thus ensuring a comparable energy density with other fuels. Its high octane rating is a beneficial feature for its use in boosted Spark-Ignition (SI) engines. Even though early studies on ammonia use as an internal combustion engine (ICE) fuel are reported [4–6], a broad commercial deployment was first hindered by its difficult flammability and very low combustion intensity, illustrated by its narrow flammability limits and low Laminar Burning Velocity (LBV) in Table 1, respectively.

**Table 1.** Ammonia properties and comparison with other fuels at 300 K and 0.1 MPa. Data from [7–9]

	Ammonia	Methanol	Hydrogen	Methane	Gasoline
Formula	NH <sub>3</sub>	CH <sub>3</sub> OH	H <sub>2</sub>	CH <sub>4</sub>	-
Storage	Liquid	Liquid	Compressed	Compressed	Liquid
Storage temperature (K)	300	300	300	300	300
Storage pressure (MPa)	1.1	0.1	70	25	0.1
Density under storage conditions (kg.m <sup>-3</sup> )	600	784.6	39.1	187	~740
Lower Heating Value (LHV) (MJ/kg)	18.8	19.9	120	50	44.5
LBV @ $\phi = 1$ (m.s <sup>-1</sup> )	0.07	0.36	3.51	0.38	0.58
Auto-ignition temp. (K)	930	712	773-850	859	503
Research Octane Number	130	119	>100	120	90-98
Flammability limits in air (vol.%)	15-28	6.7-36	4.7-75	5-15	0.6-8

Several research groups are carrying investigations to assess the best methods to compensate ammonia's poor combustion properties, as summarized recently by Valera-Medina et al. [9]. A wide variety of technical applications and conditions were already tested, including compression- and spark-ignition ICEs, as well as gas turbines (GT), with direct or indirect ammonia injection as a single or dual fuel in gaseous or liquid phase. Kobayashi et al. [10] focused their recent study on NH<sub>3</sub> combustion in swirl combustors producing low nitrogen oxides (NO<sub>x</sub>) for GT applications. Similarly, Pugh et al. [11] investigated the benefits of steam addition and elevated ambient conditions on NO<sub>x</sub> emissions from NH<sub>3</sub>/H<sub>2</sub>/air in a swirl burner. The dual fuel approach was also widely experimentally studied in compression-ignition engines, using kerosene, diesel, dimethyl-ether or hydrogen from ammonia dissociation as a pilot fuel to promote the auto-ignition [10-15]. Significant carbon-based emission reduction can be achieved at comparable power performances by NH<sub>3</sub> blend under certain conditions. NO<sub>x</sub> emissions from NH<sub>3</sub>-diesel dual fuel could be reduced for NH<sub>3</sub> energy content in the fuel less than 40% [13].

Aiming at using NH<sub>3</sub> as a main fuel for further decarbonization, and in order to take advantage of its high octane rating, the spark-ignition is seen as a meaningful method to initiate the combustion in ICEs. Granell et al. [18-19] fueled a CFR engine with ammonia and gasoline/air premixture. They determined the optimal NH<sub>3</sub>/gasoline proportions for stable and knock-free operating modes as a function of compression ratios (CR). A 70% NH<sub>3</sub> / 30% gasoline blend by energy was given as a good trade-off at full load, while neat gasoline is required

at idle. The authors suggested to use supercharged operation instead of increasing the CR for the given chamber geometry, since  $\text{NH}_3$  requires an early SI timing. Engine-out  $\text{NH}_3$  emissions were mostly proportional to the intake  $\text{NH}_3$  concentration and reached 22000 ppmvw for a stoichiometric  $\text{NH}_3$ /air mixture at the recommended 10:1 CR. HC and CO emissions decreased as a function of  $\text{NH}_3$  amount, as well as  $\text{NO}_x$  emissions (slightly) around 2500 ppmvw. Ryu et al. [20], from similar studies in a CFR engine (CR = 10:1) tested direct gaseous  $\text{NH}_3$  injection with gasoline. The range for acceptable injection pressure allowing overcoming in-cylinder pressure while avoiding  $\text{NH}_3$  liquefaction is narrow, because of its low vaporization pressure. The best power output was achieved for advanced  $\text{NH}_3$  injection timing and increased injection duration. The brake specific energy consumption (BSEC) was unchanged with ammonia addition, regardless of the load.  $\text{NO}_x$  and  $\text{NH}_3$  emissions increased strongly with the intake  $\text{NH}_3$  amount and the load. They suggested also to partially dissociate ammonia in  $\text{H}_2$  and  $\text{N}_2$  prior to direct injection with gasoline and air in the same CFR engine [21]. The combustion efficiency was significantly increased and the BSEC and the N-based emissions were accordingly reduced, especially at low loads. Ammonia combustion enhancement by in-situ  $\text{NH}_3$  dissociation was also investigated by Frigo et al. [22] not in a CFR but in a commercial two-cylinder SI engine (CR = 10.7:1) equipped with a dedicated catalytic reformer. The stability of the whole system was proven for stoichiometric mixtures over a range of engine speeds and loads. A minimum hydrogen-to-ammonia energy ratio of 7% at full load and 11% at half load was injected, and could be achieved when operating the reformer. They suggested increasing the CR or setting-up a tailored ignition system for cold start.  $\text{NO}_x$  emissions were found to be quite low with a maximum around 1700 ppm at full load and 3000 rpm. In [23], the same authors reported  $\text{NH}_3$  emissions surprisingly under 100 ppm. Mørch et al. [8] similarly studied  $\text{NH}_3/\text{H}_2$  blends fueled in a SI engine (CFR) at various CR with  $\text{NH}_3$  provided from in-situ heat-assisted desorption from a metal ammine complex. They reported an increased efficiency compared with gasoline operation due to the possibility of knock-free CR increase. The best performance was found at stoichiometry for 10 vol.%  $\text{H}_2$  in the fuel, since higher hydrogen fractions certainly induce higher wall heat losses. At this operating point, the authors recommended the use of Selective Catalytic Reduction (SCR) to eliminate the significant  $\text{NO}_x$  exhaust fraction (1500 ppm), similar to the one observed for gasoline operation. This could be done conveniently, since ammonia is available in-situ. A focus on N-based pollutant emissions from a 80 vol.%  $\text{NH}_3$  / 20 vol.%  $\text{H}_2$  fueled CFR engine was proposed by Westlye et al. [24]. In that study, NO emissions showed a leaner peak than for gasoline, but with similar magnitude. Higher  $\text{NO}_2$  emissions than with gasoline were reported but accounting for a low share around 3-4% of the total  $\text{NO}_x$ .  $\text{N}_2\text{O}$  emissions due to flame temperatures below 1400 K were sufficiently low at maximal brake torque (MBT). Reduced  $\text{NO}_x$  emissions can thus be achieved near stoichiometric conditions.  $\text{NH}_3$  slip of several hundreds of ppm is observed in the exhaust and explained by a rapid hydrogen flame propagation followed by a bulk combustion, while some ammonia is trapped in the piston crevices and cannot fully burn. Higher CR causes the increase of both  $\text{NO}_x$  and  $\text{NH}_3$  emissions. Westlye et al. also demonstrated the feasibility of SCR systems as a function of the exhaust temperature and  $\text{NO}_x$  to  $\text{NH}_3$  ratio.

Therefore, a strong evidence of the suitability of ammonia as a low-carbon SI engine fuel is reported in the literature. In order to consolidate those findings and transpose them in recent SI engine designs, the present work introduces the first measurements of an ongoing systematic experimental study on premixed  $\text{NH}_3/\text{H}_2$ /air combustion in a PSA four-valves GDI engine. In the first part, the experimental setup is introduced, as well as the methodology to estimate the laminar burning velocity. New measurement data from engine experiments in a commercial engine are then presented and discussed. The influence of the hydrogen fuel fraction, the fuel/air equivalence ratio and the engine load on the combustion efficiency, engine performance and

pollutant emissions is investigated. As a governing parameter for classical SI combustion mode, the influence of the mixtures LBV at spark timing is assessed.

### Experimental setup and operating conditions

Experiments are carried out in a commercial four-cylinder four-stroke SI engine modified to a single-cylinder engine by fueling only one out of four cylinders. Table 2 presents the engine specifications.

**Table 2.** Engine specifications

Model	PSA EP6DT
Stroke	85.8 mm
Bore	77 mm
Connecting rod length	138.5 mm
Displacement volume	399.5 cm <sup>3</sup>
Compression ratio	10.5:1
Valves	4
Engine speed	1500 rpm

The engine is driven by an electric motor at a fixed engine speed of 1500 rpm. The main shaft is equipped with an optical encoder for angular position monitoring with a 0.1 Crank Angle Degree (CAD) resolution. The TDC of the compression stroke is taken as zero reference for the angular position, therefore expressed in CAD after TDC ( $^{\circ}$ ATDC) in the following. Engine intake and exhaust temperature and pressure are monitored using type K thermocouples and piezo-resistive absolute pressure transducers. A water-cooled AVL piezoelectric pressure transducer with a 0.1 CAD resolution provides in-cylinder pressure measurements. Its measuring range is 0 – 25 MPa. The absolute cylinder pressure is obtained by equalizing the in-cylinder pressure and the mean absolute intake pressure ( $P_{in}$ ) 20 CAD after inlet valve opening. The spark plug used is the original one with a time discharge set to 2 ms. All gaseous flows are measured and controlled using Brooks thermal mass flowmeters with  $\pm 0.7\%$  accuracy, pre-heated to the intake temperature of 323 K and premixed in an intake plenum before injection. A scheme of the experimental setup is shown in Figure 1.

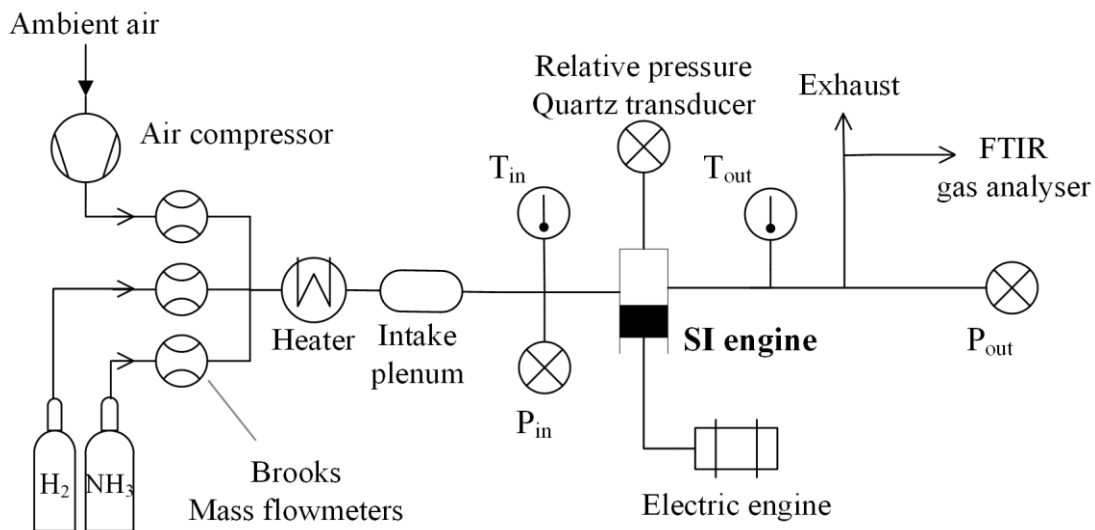
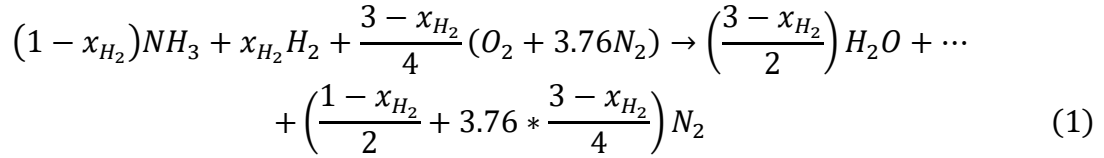


**Figure 1.** Scheme of the experimental setup

The global stoichiometric reaction of  $\text{NH}_3/\text{H}_2/\text{air}$  combustion is as:



with  $x_{\text{H}_2}$ , the hydrogen molar fraction in the fuel mixture. Non-stoichiometric mixtures are defined by the global fuel-air equivalence ratio,  $\phi$ :

$$\phi = \frac{\frac{X_{\text{H}_2} + X_{\text{NH}_3}}{X_{\text{air}}}}{\left(\frac{X_{\text{H}_2} + X_{\text{NH}_3}}{X_{\text{air}}}\right)_{st}} \quad (2).$$

$X_s$  represents the molar fraction of the species  $s$  in the reactive mixture. The stoichiometric air/fuel ratio by mass is around 6 for neat  $\text{NH}_3$  fuel and thus about twice smaller than for gasoline. The range of investigated operating conditions is summarized in Table 3. The spark-ignition timing is set at maximum brake torque (MBT) to ensure the maximum net indicated mean effective pressure (IMEP<sub>n</sub>), a quantification of the work provided by the combustion in the absence of direct torque measurements. The friction losses caused by the three deactivated pistons make the latter irrelevant. The engine is operated at full load ( $P_{in} = 100$  kPa) and under slightly supercharged conditions ( $P_{in} = 120$  kPa). Partial load operation will be investigated in future work. Cycle-to-cycle variability is considered by recording 100 consecutive pressure cycles for each test. Averaged values over 100 cycles are presented in this paper. The exhaust gases are analyzed using a Gasmet Fourier Transform Infrared (FTIR) spectrometer, allowing the NO<sub>x</sub> and NH<sub>3</sub> emissions measurement.

**Table 3.** Overview of the operating test conditions.  
 $e_{\text{H}_2}$ : H<sub>2</sub> energy fraction in the total energy amount (based on LHV)

Intake temperature (K)	Intake pressure (kPa)	$x_{\text{H}_2}$	$e_{\text{H}_2}$	$\phi$	SI timing
323	{100; 120}	[0 – 0.6]	[0 – 0.54]	[0.6 – 1.2]	MBT

### Combustion analysis and laminar burning velocity calculation

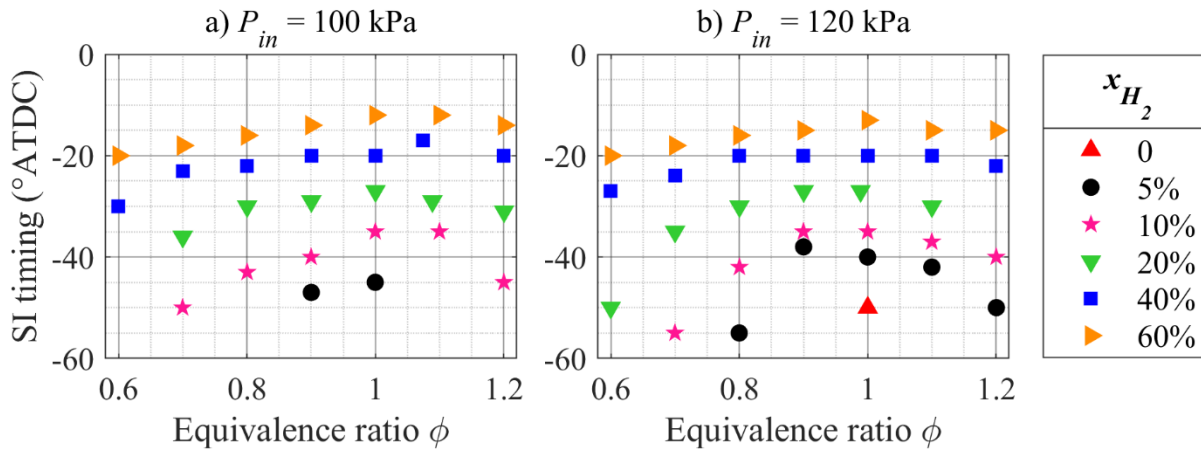
A delayed crank angle phasing and thermodynamic losses can cause top dead center (TDC) detection and CR errors during the compression stroke. Therefore, the methodology proposed by Tazerout et al. [25-26] for pressure – volume lag elimination is implemented within the classical analysis of the cylinder pressure – volume data proposed by Heywood [27], neglecting crevices effects. Performance indicators such as the IMEP<sub>n</sub> and its coefficient of variation over 100 cycles (COV(IMEP<sub>n</sub>)) can be deduced accurately, as well as the bulk in-cylinder temperature. It is determined assuming mass conservation inside the cylinder after inlet valve closing. Combustion analysis is also performed based on the in-cylinder pressure by calculating the net heat release rate (HRR). This is done using a one-zone model with weighted constant-pressure heat capacity regarding the estimated burned and unburned mass fractions over time. The gross HRR from the combustion is estimated by considering the wall heat losses by means of the model of Hohenberg [28]. Combustion phasing in the cycle is established by assessing the crank

angles at which 10%, 50% and 90% of the cumulated gross heat release is reached, yielding CA10, CA50 and CA90, respectively.

The laminar burning velocity of the reactive mixtures under SI timing thermodynamic conditions is calculated by means of a newly developed LBV correlation proposed by Goldmann and Dinkelacker [29] on the basis of the detailed reaction mechanism of Mathieu and Petersen [30]. This correlation takes the presence of hydrogen in the fuel into account and was validated against measurements at normal temperature and up to 500 kPa of pressure for various mixture compositions.

## Results and discussion

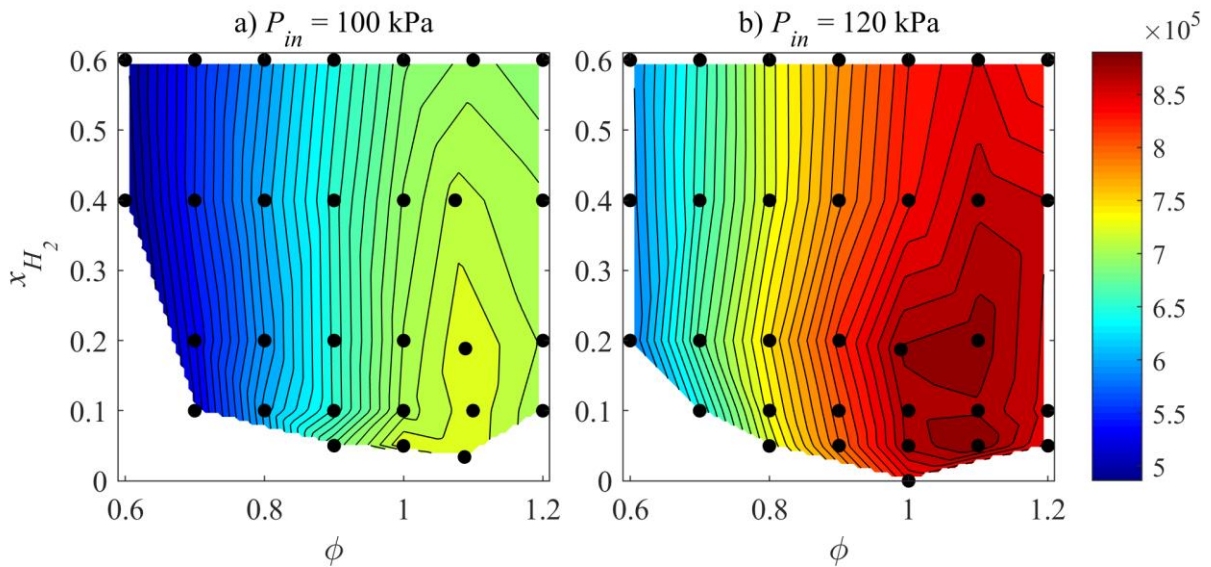
The engine operated successfully with an excellent cycle-to-cycle stability for a wide range of  $H_2$  fractions and equivalence ratios. The acceptable stability boundary was set at  $COV(IMEP_n) \leq 5\%$ , but most of the conditions showed  $COV(IMEP_n) \leq 3\%$ . It should be emphasized here that stable operation could be achieved for a stoichiometric  $NH_3$ /air mixture for  $P_{in} = 120$  kPa. Only mixtures with high hydrogen fraction were found suitable for very lean operation. Advancing the SI timing is required to reach MBT, and thus achieve optimal power output for a given condition as shown in Fig. 2. Mixtures with high  $NH_3$  content unsurprisingly require more advance due to lower LBVs and the influence of  $\phi$  is bell-shaped. For a given fuel blend, the latest optimal SI timing is located near stoichiometry, corresponding to an ignition close to TDC.



**Figure 2.** Optimized SI timing VS equivalence ratio and  $H_2$  content for two load conditions.

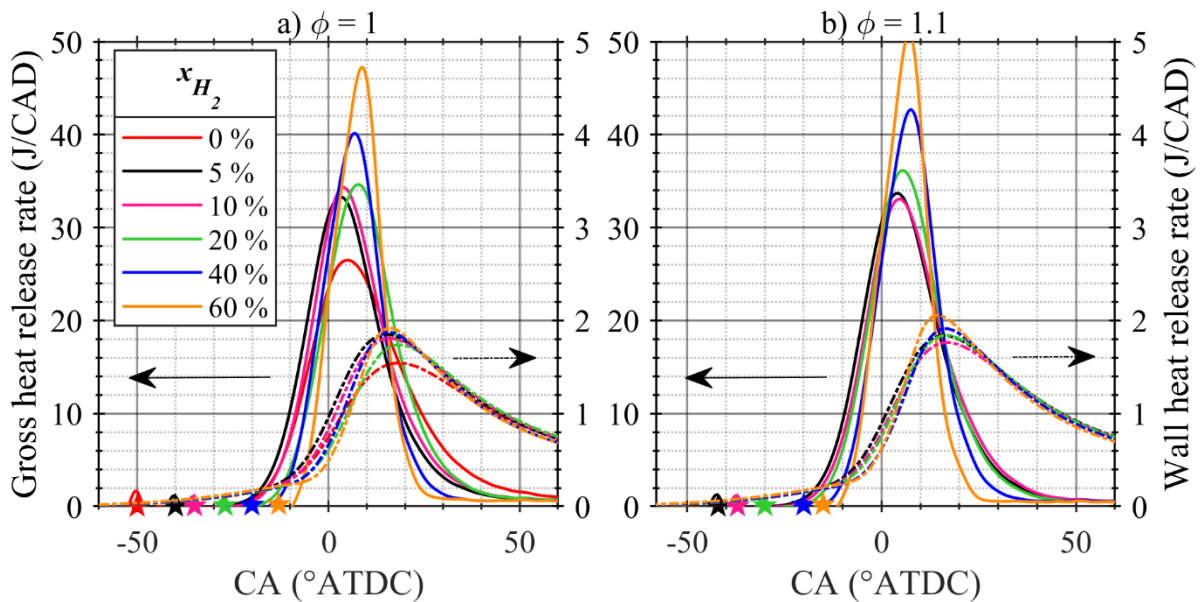
The best power output, given by the  $IMEP_n$ , is observed for supercharged operation, as shown in Fig. 3, with a maximum obtained for low to moderate hydrogen fractions up to 20% and slightly rich equivalence ratios around 1.1. The influence of the equivalence ratio is mainly correlated with the LBV, as discussed later. The influence of the  $H_2$  fraction is consistent with the observations in [8] and the power decrease at higher fractions is assumedly caused by higher wall heat losses due to higher flame temperatures.

Figure 4 shows the gross and wall heat release rates for stoichiometric (a) and slightly rich (b)  $NH_3/H_2$ /air mixtures. Mixtures with higher  $H_2$  fractions exhibit higher and narrower gross HRR peaks in spite of later ignition, confirming the higher intensity of the combustion. The wall HRR shows a trend of higher heat losses for higher  $x_{H_2}$  during the combustion phase. Care should however be taken, since SI timings are not constant and the modeled wall HRR values are quite small.



**Figure 3.** Indicated mean effective pressure measured for various mixture compositions. Circles: experimental conditions. Color contours (see online version): IMEP<sub>n</sub> in Pa, from low values (top-left, blue) to high values (bottom-right, red).

The influence of the laminar burning velocity of the mixture at SI timing on the IMEP<sub>n</sub> is shown in Fig. 5a and 5b, along with the indicated efficiencies, defined as output-to-input power ratio on an IMEP<sub>n</sub> and LHV basis, respectively. The IMEP<sub>n</sub> depends quasi - monotonically on the LBV. More specifically, at constant  $x_{H_2}$ , the IMEP<sub>n</sub> increases with increasing LBV, while it decreases for increasing  $x_{H_2}$  at constant LBV. This indicates no or little beneficial effect of the LBV bonus provided by H<sub>2</sub> on the global thermal efficiency of NH<sub>3</sub>/H<sub>2</sub>/air mixtures combustion in SI engines, since the highest power yields are reached for low LBVs.

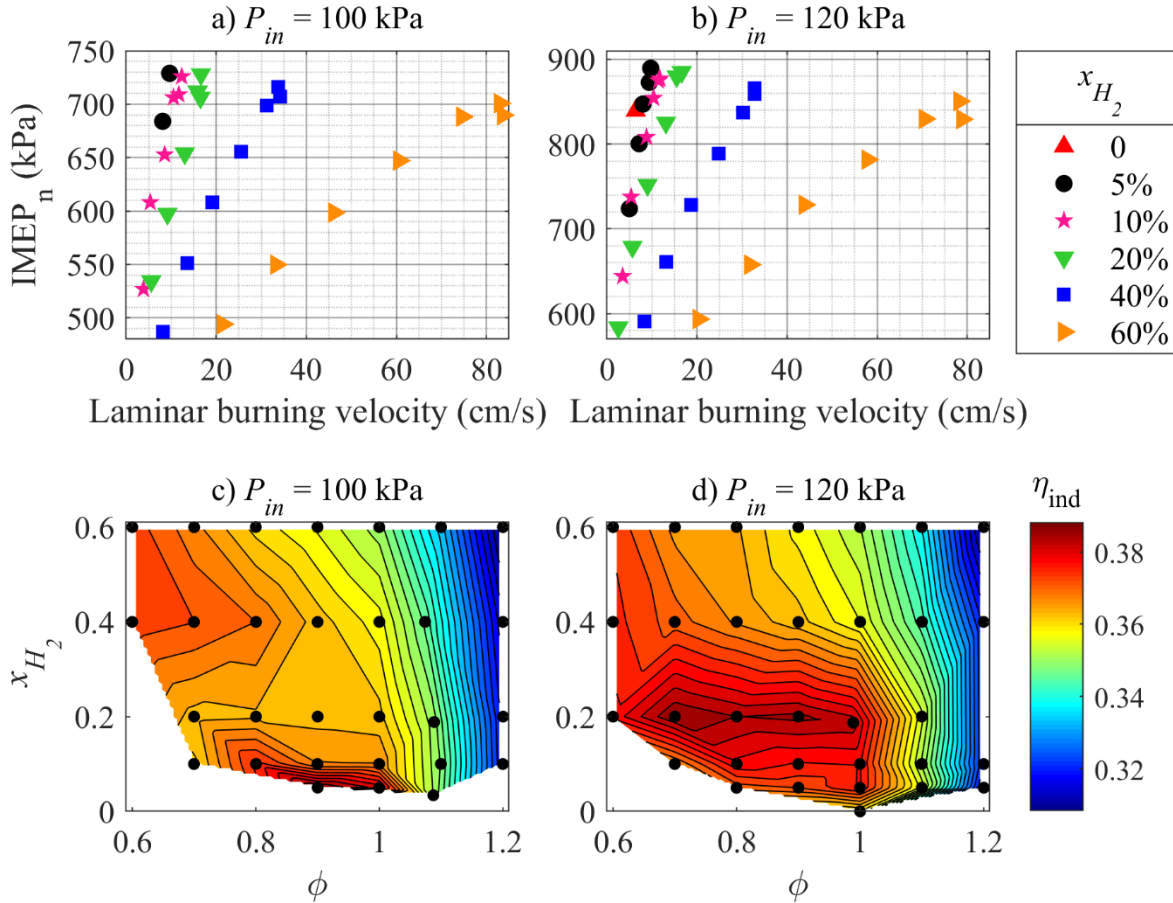


**Figure 4.** Gross heat release rate (left axis, solid lines) and wall heat release rate (right axis, dash-dotted lines) at  $P_{in} = 120$  kPa. Symbols: SI timing. Colored version online.

This is confirmed by Figure 5c and 5d, where the indicated efficiency is shown as a function of the mixture composition. The highest efficiencies are reached under slightly lean conditions for low to moderate H<sub>2</sub> fractions, in regions of diminished LBVs, which generally peaks around

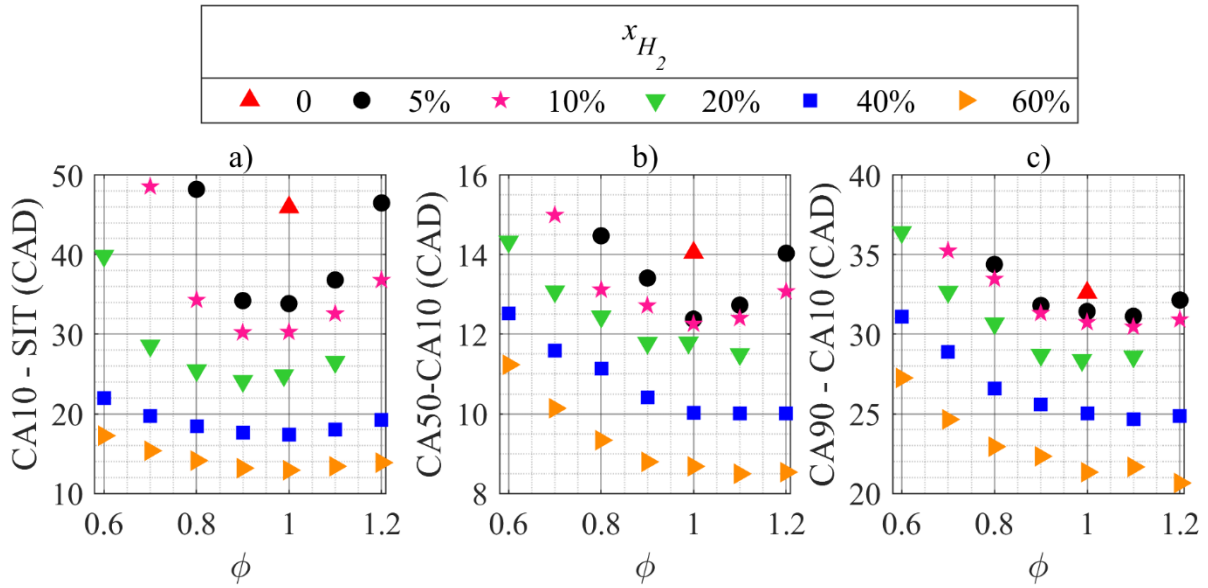


$\phi = 1.1$ . Furthermore, the benefits of flame stretch effects could explain the ability to ignite and burn with satisfying efficiency very lean mixtures with moderate  $H_2$  fraction. For example, a 80% $NH_3$  / 20% $H_2$  blend exhibits a fuel Lewis number of 0.88 at  $\phi = 0.6$  and  $P_{in} = 120$  kPa, calculated with the method in [31] and indicating a beneficial flame stretch sensitivity for the early flame propagation. Increased engine load seems to promote the indicated efficiency at moderate  $H_2$  fractions.



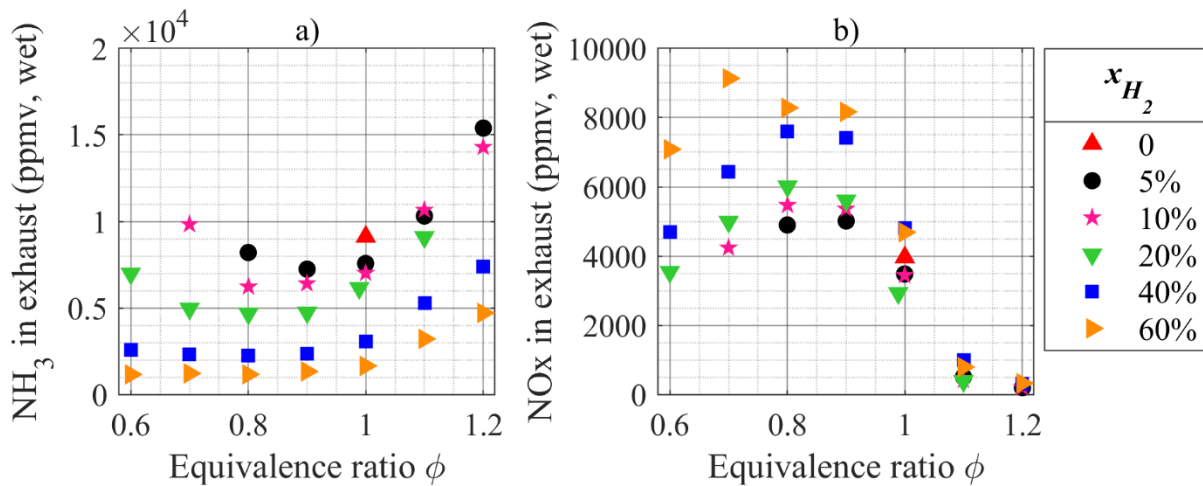
**Figure 5.** a) and b): Indicated mean effective pressure versus calculated LBV of the mixtures under SI timing conditions. c) and d): Indicated efficiency  $\eta_{ind}$  as function of the mixture.

Figure 6 further strengthens the assumption of the primary beneficial influence of  $H_2$  as an ignition promoter. The combustion phasing at  $P_{in} = 120$  kPa is shown in three steps, corresponding to the initiation phase, the propagation phase until 50% of mass burned and the bulk combustion duration. For the near stoichiometric mixtures, the initiation and the propagation are the fastest phases, while the bulk combustion duration is minimal above stoichiometry, consistently with the observations on the maximal  $IMEP_n$ . This suggests that the indicated efficiency is governed by the early stages of the combustion process, while the power output is mainly associated with the overall combustion duration. Hydrogen addition is observed to generally accelerate the combustion process and to shift the minimal durations towards richer mixtures, thus leading to shorter phases. It is especially noticeable during the initiation phase in Fig. 6a, where a 5 vol.%  $H_2$  addition ( $\sim 4\%$  by energy) causes a 26% drop in CA<sub>10</sub>-SI timing at stoichiometry. However, those considerations are not absolute as optimal SI timings were used in this study (10 CAD difference in the latter example), influencing the thermodynamic conditions at ignition.



**Figure 6.** Combustion phasing at  $P_{in} = 120$  kPa. a) Initiation phase. b) Propagation phase. c) Bulk combustion duration.

In order to wrap-up this analysis, pollutant exhaust emissions are shown in Figure 7. Only the measurements for an intake pressure of 120 kPa are depicted, since no qualitative difference with the other case was observed.  $NH_3$  emissions increase monotonically with the  $NH_3$  fraction in the fuel, as shown in Fig. 7a. Minimal emissions are observed for near-stoichiometric lean conditions, tending towards leaner mixtures as  $H_2$  is added. That observation might be linked with the better  $\eta_{ind}$  and faster combustion initiation phase under such conditions. When the equivalence ratio is increased above stoichiometry, the emissions increase significantly, reaching very high values of more than 15,000 ppmv. Heading towards very lean mixtures, the  $NH_3$  emissions increase as well, because of a likely poor combustion efficiency.



**Figure 7.** Pollutant emissions in exhaust at  $P_{in} = 120$  kPa. a) Unburned  $NH_3$ . b) Total NOx.

NOx emissions are shown in Fig. 7b. Minimal values are obtained for rich mixtures with high ammonia content. Mixtures with high  $H_2$  fuel fractions exhibit the highest emissions, probably due to higher flame temperatures that promote thermal NOx formation. Maximal values are found for equivalence ratio 0.8-0.9, as could be expected due to the presence of excess oxygen. Very high values up to 9000 ppm are observed at lean conditions, while low values

well below 500 ppm are seen at rich conditions, possibly after partial recombination with unburned  $\text{NH}_3$  in the exhaust pipe. Either way, mitigation strategies are required in order to render ammonia acceptable as a fuel for commercial applications. These could be achieved by means of a SCR catalyst, since both heat and  $\text{NH}_3$  reducing agent are available in the exhaust, as demonstrated by Westlye et al. [24].

## Conclusion

Experiments were conducted in a modern SI engine in order to assess the feasibility and the characteristics of ammonia combustion at various additional hydrogen fractions, equivalence ratios and intake pressures. In future applications, hydrogen could be provided by in-situ  $\text{NH}_3$  dissociation in a catalytic reformer. The main conclusions are as follow:

- A new measurement database of performance and emission data is provided for numerical validation purposes.
- $\text{NH}_3$  is confirmed as a very suitable SI engine fuel for modern engines since neat ammonia operation could be achieved under supercharged conditions, even slight ones.
- Highest power output and indicated efficiency were achieved at low and moderate hydrogen addition, at slightly fuel-rich and slightly fuel-lean conditions respectively. Supercharged operation leads to improved power yield and efficiency.
- Hydrogen is primarily an ignition promoter, allowing significant performance and stability improvement when added in small quantities, mainly beneficial for the early stages of the combustion. Bulk ammonia combustion assumedly provides most of the useful energy. Wall heat losses are thought to play a significant role at high hydrogen fractions.
- High  $\text{NO}_x$  and  $\text{NH}_3$  emissions need to be mitigated in future applications.

Therefore, a trade-off needs to be found between power output, efficiency and pollutant emissions. This could be achieved near stoichiometric conditions, thanks to a  $\text{NO}_x$  selective catalytic reduction with  $\text{NH}_3$  slip at the exhaust or by a recirculation and a thermo-catalytic reforming of a part of unburned  $\text{NH}_3$  to generate small but sufficient  $\text{H}_2$  addition. Supercharged operation is expected to be beneficial in all cases, while increasing the compression ratio remains an open question. In that matter, the interest of engine design modification for optimal  $\text{NH}_3$  fuel operation needs to be assessed.

## Nomenclature

$e_{\text{H}_2}$  Hydrogen energy fraction in the fuel blend

$P$  Pressure

$T$  Temperature

$x_{\text{H}_2}$  Hydrogen mole fraction in the fuel blend

Greek letters

$\eta_{\text{ind}}$  Indicated efficiency

$\phi$  Fuel/air equivalence ratio

Subscripts

in Intake

out Exhaust

## References

- [1] Rogelj, J., Shindell, D., Jiang, K., Fifita, S., Forster, P., Ginzburg, V. et al., "Mitigation Pathways Compatible with 1.5°C in the Context of Sustainable Development", In: *Global warming of 1.5°C. An IPCC Special Report on the impacts of global warming of 1.5°C above pre-industrial levels and related global greenhouse gas emission pathways, in the context of strengthening the global response to the threat of climate change,*

- sustainable development, and efforts to eradicate poverty*, (2018).
- [2] International Energy Agency, *Technology Roadmap Energy storage*, (2014).
  - [3] Tatin, A., Bonin, J., Robert, M., "A Case for Electrofuels", *ACS Energy Lett.* 1062–1064 (2016).
  - [4] Cornelius, W., Huellmantel, L.W., Mitchell, H.R., "Ammonia as an engine fuel", *SAE Tech. Pap.* 650052 (1965).
  - [5] Starkman, E.S., Newhall, H.K., Sutton, R., Maguire, T., Farbar, L., "Ammonia as a Spark Ignition Engine Fuel: Theory and Application", *SAE Tech. Pap.* 660155 (1966).
  - [6] Gray, J.T.J., Dimitroff, E., Meckel, N.T., Quillian, R.D.J., "Ammonia Fuel - Engine Compatibility and Combustion", *SAE Tech. Pap.* 660156 (1966).
  - [7] Linstrom, P.J., Mallard, W.G., *NIST Chemistry WebBook, NIST Standard Reference Database Number 69*, National Institute of Standards and Technology, n.d.
  - [8] Mørch, C.S., Bjerre, A., Gøttrup, M.P., Sorenson, S.C., Schramm, J., "Ammonia/hydrogen mixtures in an SI-engine: Engine performance and analysis of a proposed fuel system", *Fuel* 90: 854–864 (2011).
  - [9] Valera-Medina, A., Xiao, H., Owen-Jones, M., David, W.I.F., Bowen, P.J., "Ammonia for power", *Prog. Energy Combust. Sci.* 69: 63–102 (2018).
  - [10] Kobayashi, H., Hayakawa, A., Somarathne, K.D.D.K.A., Okafor, E.C., "Science and technology of ammonia combustion", *Proc. Combust. Inst.* 37, 109-133 (2019).
  - [11] Pugh, D., Bowen, P., Valera-Medina, A., Giles, A., Runyon, J., Marsh, R., "Influence of steam addition and elevated ambient conditions on NO<sub>x</sub> reduction in a staged premixed swirling NH<sub>3</sub>/H<sub>2</sub> flame", *Proc. Combust. Inst.* 37, 5401-5409 (2019).
  - [12] Reiter, A.J., Kong, S.C., "Demonstration of compression-ignition engine combustion using ammonia in reducing greenhouse gas emissions", *Energy and Fuels.* 22: 2963–2971 (2008).
  - [13] Reiter, A.J., Kong, S.C., "Combustion and emissions characteristics of compression-ignition engine using dual ammonia-diesel fuel", *Fuel* 90: 87–97 (2011).
  - [14] Gill, S.S., Chatha, G.S., Tsolakis, A., Golunski, S.E., York, A.P.E., "Assessing the effects of partially decarbonising a diesel engine by co-fuelling with dissociated ammonia", *Int. J. Hydrogen Energy* 37: 6074–6083 (2012).
  - [15] Gross, C.W., Kong, S.C., "Performance characteristics of a compression-ignition engine using direct-injection ammonia-DME mixtures", *Fuel* 103: 1069–1079 (2013).
  - [16] Ryu, K., Zacharakis-Jutz, G.E., Kong, S.-C., "Performance characteristics of compression-ignition engine using high concentration of ammonia mixed with dimethyl ether", *Appl. Energy* 113: 488–499 (2014).
  - [17] Pochet, M., Truedsson, I., Foucher, F., Jeanmart, H., Contino, F., "Ammonia-Hydrogen blends in Homogeneous-Charge Compression-Ignition Engine", *SAE Tech. Pap.* 2017-24-0087 (2017).
  - [18] Grannell, S.M., Assanis, D.N., Bohac, S. V., Gillespie, D.E., "The Fuel Mix Limits and Efficiency of a Stoichiometric, Ammonia, and Gasoline Dual Fueled Spark Ignition Engine", *J. Eng. Gas Turbines Power* 130: 042802-1-8 (2008).
  - [19] Grannell, S.M., Assanis, D.N., Gillespie, D.E., Bohac, S. V., "Exhaust Emissions From a Stoichiometric, Ammonia and Gasoline Dual Fueled Spark Ignition Engine", *Proc. ASME Intern. Combust. Engine Div.*, Milwaukee, Wisconsin, USA, paper ICES2009-76131 (2009).
  - [20] Ryu, K., Zacharakis-Jutz, G.E., Kong, S.-C., "Effects of gaseous ammonia direct injection on performance characteristics of a spark-ignition engine", *Appl. Energy* 116: 206–215 (2014).
  - [21] Ryu, K., Zacharakis-Jutz, G.E., Kong, S.C., "Performance enhancement of ammonia-fueled engine by using dissociation catalyst for hydrogen generation", *Int. J. Hydrogen*

- Energy* 39: 2390–2398 (2014).
- [22] Frigo, S., Gentili, R., "Analysis of the behaviour of a 4-stroke Si engine fuelled with ammonia and hydrogen", *Int. J. Hydrogen Energy* 38: 1607–1615 (2013).
  - [23] Comotti, M., Frigo, S., "Hydrogen generation system for ammonia-hydrogen fuelled internal combustion engines", *Int. J. Hydrogen Energy* 40: 10673–10686 (2015).
  - [24] Westlye, F.R., Ivarsson, A., Schramm, J., "Experimental investigation of nitrogen based emissions from an ammonia fueled SI-engine", *Fuel* 111: 239–247 (2013).
  - [25] Tazerout, M., Le Corre, O., Stouffs, P., "Compression Ratio and TDC calibrations using Temperature - Entropy Diagram", *SAE Tech. Pap.* 1999-01-3509 (1999).
  - [26] Tazerout, M., Le Corre, O., Rousseau, S., "TDC Determination in IC Engines Based on the Thermodynamic Analysis of the Temperature-Entropy Diagram", *SAE Tech. Pap.* 1999-01-1489 (1999).
  - [27] Heywood, J.B., *Internal Combustion Engine Fundamentals*, McGraw-Hill, 1988.
  - [28] Hohenberg, G., "Advanced approaches for heat transfer calculations", *SAE Tech. Pap.* 790825 (1979).
  - [29] Goldmann, A., Dinkelacker, F., "Approximation of laminar flame characteristics on premixed ammonia/hydrogen/nitrogen/air mixtures at elevated temperatures and pressures", *Fuel* 224: 366–378 (2018).
  - [30] Mathieu, O., Petersen, E.L., "Experimental and modeling study on the high-temperature oxidation of Ammonia and related NO<sub>x</sub> chemistry", *Combust. Flame* 162: 554–570 (2015).
  - [31] Lapalme, D., Lemaire, R., Seers, P., "Assessment of the method for calculating the Lewis number of H<sub>2</sub>/CO/CH<sub>4</sub> mixtures and comparison with experimental results", *Int. J. Hydrogen Energy* 42: 8314–8328 (2017).